

1 *Supporting Information for*

2 **An Overlooked Kinetic Relaxation in the Formation of Sesquiterpene-Derived**
3 **Criegee Intermediates**

4

5 Hengjia Ou,^{1,†} Yao Li,^{2,†} Yuqing Sha,³ Hui Zhou,^{4,5} Jingkun Jiang,⁶ Kunpeng Chen^{4,6,*}

6

7 ¹Guangzhou Institute of Tropical and Marine Meteorology of China Meteorological
8 Administration, Guangzhou 510640, China

9 ²Yantai Meteorological Bureau, Yantai, Shandong 264003, China

10 ³Fuyang Meteorological Bureau, Fuyang, Anhui 236000, China

11 ⁴Key Laboratory for Thermal Science and Power Engineering of Ministry of Education, Beijing
12 Key Laboratory of CO₂ Utilization and Reduction Technology, Department of Energy and Power
13 Engineering, Tsinghua University, Beijing 100084, China

14 ⁵Shanxi Research Institute for Clean Energy, Tsinghua University, Shanxi, Taiyuan 030000, China

15 ⁶State Key Laboratory of Regional Environment and Sustainability, School of Environment,
16 Tsinghua University, Beijing 100084, China

17

18 Email: chenkp@mail.tsinghua.edu.cn

19

20 [†]Hengjia Ou and Yao Li contributed equally to this work.

21

22 Texts: S1 to S2

23 Tables: S1 to S4

24 Figures: S1 to S9

25

26 **Text S1.** Derivation of the formation rate constant of CIs

27 This section describes the detailed derivation for the formation rate constant of CIs. For
28 simplicity in the derivation, we firstly consider one CI from the ozonolysis of the sesquiterpene
29 (SQT) molecule, wherein only one SPC and one POZ connect the reaction chain (Scheme II in the
30 manuscript). For atmospheric chemistry models, the formation rate of CIs (R_f) is typically given
31 by Eq. (S1).

$$32 \quad R_f = k_{CI} \cdot C_{SQT} \cdot C_{O_3} \quad (S1)$$

33 Here k_{CI} is the formation rate constant of CIs generated from the reactions between
34 sesquiterpene (SQT) and O_3 , while C_{SQT} and C_{O_3} represent the concentrations of SQT and O_3 . If
35 we change the perspective and start to think about the basic principle of elementary reactions, R_f
36 is actually determined by the rate of POZ decomposition (Scheme II in the manuscript), and its
37 expression is given by Eq. (S2).

$$38 \quad R_f = k_3 \cdot C_{POZ} \quad (S2)$$

39 If we try to compare Eq. (S2) with Eq. (S1), we will find it necessary to express the
40 concentration of POZ (C_{POZ}) as a function of C_{SQT} and C_{O_3} . Based on Scheme II in the manuscript,
41 the kinetics regarding the change of C_{POZ} along with ozonolysis time (t) can be analytically
42 expressed as Eq. (S3).

$$43 \quad \frac{dC_{POZ}}{dt} = k_2 \cdot C_{SPC} - (k_{-2} + k_3) \cdot C_{POZ} \quad (S3)$$

44 The quantity C_{SPC} represents the concentration of SPC and k_2 is the rate constant of POZ
45 formation from the SPC. The generated POZ can either reversely produce SPC again or decompose
46 into the CI, with the rate constants represented by k_{-2} and k_3 , respectively. As supported by
47 experimental studies (Talukdar et al., 2003; Davis et al., 2005; Ou and Chen, 2025), C_{SPC} can be
48 approximated by its steady-state concentration (Eq. (S4)).

49
$$\frac{dC_{SPC}}{dt} = 0 \quad (S4)$$

50 Eq. (S4) means that, at any time during the SQT ozonolysis, the concentration of the SPC
 51 is assumed to be constant. The left-hand side of Eq. (S4), based on Scheme II in the manuscript,
 52 can be expressed as Eq. (S5).

53
$$\frac{dC_{SPC}}{dt} = k_1 \cdot p \cdot C_{SQT} \cdot C_{O_3} - (k_{-1} + k_2) \cdot C_{SPC} \quad (S5)$$

54 Here k_1 is the rate constant of effective collisions between the SQT and O_3 , p is the
 55 branching ratio that the effective collisions can produce this SPC (as the SQT and O_3 indeed yield
 56 multiple SPCs), k_{-1} is the dissociation rate constant of the SPC, k_2 is the formation rate constant
 57 of the POZ from the SPC. Combining Eqs. (S4) and (S5), the steady-state concentration of SPC,
 58 denoted as $C_{SPC,ss}$, is given by Eq. (S6).

59
$$C_{SPC,ss} = k_1 \cdot p \cdot \left(\frac{1}{k_{-1} + k_2} \right) \cdot C_{SQT} \cdot C_{O_3} \quad (S6)$$

60 Eq. (S6) suggests that, within the modeling timescale, both the concentrations of SQT and
 61 O_3 are stable enough, so C_{SQT} and C_{O_3} remain constant. It is noted that $C_{SPC,ss}$ is a function of
 62 temperature since k_1 , k_{-1} and k_2 may change during the temperature variations. Substituting Eq.
 63 (S6) into Eq. (S3), we obtain Eq. (S7).

64
$$\frac{dC_{POZ}}{dt} = k_1 \cdot p \cdot \left(\frac{k_2}{k_{-1} + k_2} \right) \cdot C_{SQT} \cdot C_{O_3} - (k_{-2} + k_3) \cdot C_{POZ} \quad (S7)$$

65 For convenience, if we denote C_{POZ} as y , the first term on the right-hand side of Eq. (S7)
 66 as b , and $(k_{-2} + k_3)$ in Eq. (S7) as a , the Eq. (S7) then becomes a classical ordinary differential
 67 equation as shown in Eq. (S8).

68
$$\frac{dy}{dt} = b - ay \quad (S8)$$

69 After rearranging the Eq. (S8), we can conduct the indefinite integral as Eq. (S9), and then
 70 obtain the expression of y as a function of t with a constant c' for integration (Eq. (S10)).

$$71 \quad \frac{1}{a} \cdot \int \frac{d(ay)}{b-ay} = \int dt \quad (S9)$$

$$72 \quad y = \frac{b}{a} \cdot (1 - c'e^{-at}) \quad (S10)$$

73 Notably, in the experimental measurements of CI formation from ozonolysis, there is
 74 typically no pre-existing POZ (i.e., $y = 0$) when the ozonolysis starts (i.e., $t = 0$). In this case, we
 75 can obtain the value of c' by solving Eq. (S10), which provides $c' = 1$.

76 By transforming a and b back to their original symbols, the analytical expression of C_{POZ}
 77 is given by Eq. (S11).

$$78 \quad C_{POZ} = k_1 \cdot p \cdot \left(\frac{1}{k_{-2}+k_3}\right) \cdot \left(\frac{k_2}{k_{-1}+k_2}\right) \cdot [1 - e^{-(k_{-2}+k_3)t}] \quad (S11)$$

79 Substituting Eq. (S11) into Eq. (S2), the analytical expression of R_f is given by Eq. (S12).

$$80 \quad R_f = k_1 \cdot p \cdot \left(\frac{k_3}{k_{-2}+k_3}\right) \cdot \left(\frac{k_2}{k_{-1}+k_2}\right) \cdot [1 - e^{-(k_{-2}+k_3)t}] \cdot C_{SQT} \cdot C_{O_3} \quad (S12)$$

81 Now we obtain the formation rate of a single CI as a function of all the related rate constants
 82 of elemental reactions as well as the concentrations of SQT and O_3 . Considering all the SPCs and
 83 their corresponding POZs generated from the ozonolysis and all the CIs generated from POZ
 84 decomposition, Eq. (S12) can be rewritten into a comprehensive expression given by Eq. (S13).

$$85 \quad R_f = k_1 \cdot \sum_i \sum_j \left\{ p_i \cdot \left(\frac{k_{3,i,j}}{k_{-2,i}+k_{3,i,j}}\right) \cdot \left(\frac{k_{1,i} \cdot k_{2,i}}{k_{-1,i}+k_{2,i}}\right) \cdot [1 - e^{-(k_{-2,i}+k_{3,i,j})t}] \right\} \cdot C_{SQT} \cdot C_{O_3} \quad (S13)$$

86 The subscript i in Eq. (S13) indicates the i -th SPC and the i -th POZ, and the subscript j
 87 indicates the j -th CI from the i -th POZ decomposition. Both i and j are positive integers. The value
 88 of i ranges from 1 to the total number of CIs, while the value of j is either 1 or 2, since each POZ
 89 can decompose into two possible CIs. Comparing Eq. (S13) with Eq. (S1), we can directly obtain
 90 the expression of k_{CI} , which shows the rate constant of total CI formation (Eq. (S14)).

$$91 \quad k_{CI} = k_1 \cdot \sum_i \sum_j \left\{ p_i \cdot \left(\frac{k_{3,i,j}}{k_{-2,i}+k_{3,i,j}}\right) \cdot \left(\frac{k_{1,i} \cdot k_{2,i}}{k_{-1,i}+k_{2,i}}\right) \cdot [1 - e^{-(k_{-2,i}+k_{3,i,j})t}] \right\} \quad (S14)$$

92 Eq. (S14) handles all the kinetic details at the “double-well” potential energy surface of the
 93 CI formation mechanism, and we indicate that Eq. (S14) can be simplified by two approximations.
 94 The first approximation is that k_{-2} may vanish, as it is negligibly small compared to $k_{3,i,j}$. This is
 95 because the energy barriers for the decomposition of POZs into SPCs are significantly higher than
 96 those for the CI formation (Donahue et al., 2011; Vereecken and Francisco, 2012; Taatjes et al.,
 97 2014). In this case, k_{CI} can be approximated by Eq. (S15).

$$\begin{aligned}
 98 \quad k_{CI} &\approx k_1 \cdot \sum_i \sum_j \left[p_i \cdot \frac{k_{3,i,j}}{k_{3,i,j}} \cdot \left(\frac{k_{2,i}}{k_{-1,i} + k_{2,i}} \right) \cdot (1 - e^{-k_{3,i,j}t}) \right] \\
 99 \quad &= k_1 \cdot \sum_i \sum_j \left[p_i \cdot \left(\frac{k_{2,i}}{k_{-1,i} + k_{2,i}} \right) \cdot (1 - e^{-k_{3,i,j}t}) \right] \quad (S15)
 \end{aligned}$$

100 The second approximation is that the decomposition of each POZ produces only one major
 101 CI. Although there should be two CIs generated from the one POZ, one of the CIs has a faster
 102 formation rate, wherein its k_3 is typically $\sim 1-10$ orders of magnitude higher than that of the other
 103 (Fig. 3). In this case, the summation based on j vanishes so that k_{CI} can be further approximated
 104 by Eq. (S16).

$$105 \quad k_{CI} \approx k_1 \cdot \sum_i \left[p_i \cdot \left(\frac{k_{2,i}}{k_{-1,i} + k_{2,i}} \right) \cdot (1 - e^{-k_{3,i}t}) \right] \quad (S16)$$

106 The expression of k_{CI} in Eq. (S16) is very similar to the expression of k_{oz} (Eq. (1) in the
 107 manuscript). Their relationship can be clearly illustrated if we denote the branching ratio of the i -
 108 th ozonolysis channel (i.e., the reaction pathway that generates the i -th CI through the i -th SPC
 109 and the i -th POZ) as r_i , which is given by Eq. (S17).

$$110 \quad r_i = p_i \cdot \left(\frac{k_{2,i}}{k_{-1,i} + k_{2,i}} \right) / \sum_i \left[p_i \cdot \left(\frac{k_{2,i}}{k_{-1,i} + k_{2,i}} \right) \right] \quad (S17)$$

111 Eq. (S17) reveals that $\sum_i r_i = 1$. Substituting Eq. (S17) into Eq. (S16), the relationship
 112 between k_{CI} and k_{oz} can be derived as Eq. (S18).

$$\begin{aligned}
113 \quad k_{CI} &\approx k_1 \cdot \sum_i \left\{ r_i \cdot \sum_i \left[p_i \cdot \left(\frac{k_{2,i}}{k_{-1,i} + k_{2,i}} \right) \right] \cdot (1 - e^{-k_{3,i}t}) \right\} \\
114 \quad &= k_1 \cdot \sum_i \left[p_i \cdot \left(\frac{k_{2,i}}{k_{-1,i} + k_{2,i}} \right) \right] \cdot \sum_i [r_i \cdot (1 - e^{-k_{3,i}t})] \\
115 \quad &= k_{oz} \cdot \sum_i [r_i \cdot (1 - e^{-k_{3,i}t})] \tag{S18}
\end{aligned}$$

116 Eq. (S18) provides a clear physical sense that, for the i -th CI, its formation rate constant
117 can be estimated by the product of the ozonolysis rate constant and the time-dependent branching
118 ratio projecting of this CI ($f_{CI,i}$), which is given by Eq. (S19).

$$119 \quad f_{CI,i} = r_i \cdot (1 - e^{-k_{3,i}t}) \tag{S19}$$

120 Thus, the relationship between k_{CI} and k_{oz} can be written as Eq. (S20).

$$121 \quad k_{CI} \approx k_{oz} \cdot \sum_i f_{CI,i} \tag{S20}$$

122 The time dependence of $f_{CI,i}$ shows the kinetic relaxation of k_{CI} . Eqs. (S19) and (S20) reveal
123 that, when the ozonolysis begins (i.e., $t = 0$), the value of $f_{CI,i}$ is zero, which means that if the i -th
124 POZ does not pre-exist, the initial formation rate constant of the i -th CI is zero, even though the
125 ozonolysis rate constant of the SQT is the positive number k_{oz} . It is also noted that the value of $f_{CI,i}$
126 will unlimitedly approach r_i if the t is infinitely large (Eq. (S21)).

$$\begin{aligned}
127 \quad \lim_{t \rightarrow \infty} k_{CI}(t, T) &\approx \lim_{t \rightarrow \infty} [k_{oz}(T) \cdot \sum_i f_{CI,i}(t, T)] \\
128 \quad &= k_{oz}(T) \cdot \lim_{t \rightarrow \infty} \sum_i f_{CI,i}(t, T) \\
129 \quad &= k_{oz}(T) \cdot \lim_{t \rightarrow \infty} \sum_i [r_i \cdot (1 - e^{-k_{3,i}t})] \\
130 \quad &= k_{oz}(T) \cdot \sum_i r_i \\
131 \quad &= k_{oz}(T) \tag{S21}
\end{aligned}$$

132 Eq. (S21) indicates that k_{oz} represents the plateau value of k_{CI} if ozonolysis could proceed
133 indefinitely. In the real atmosphere, k_{CI} is always in a state of deviation from k_{oz} , though it
134 continuously tends toward this value.

135 **Text S2.** Formation rate constant of CIs with scale factors accounting for the pre-existing POZs

136 This section derives the analytical expression of k_{CI} if POZs pre-exist before the SQT
137 ozonolysis starts. For convenience, we still start by considering only one CI produced from its
138 corresponding POZ. The analytical expression of k_{CI} in Text S1 is derived based on the absence of
139 pre-existing POZs, so that in Eq. (S10) the value of c' equals 1. If the initial concentration of this
140 POZ is not zero, we may denote the value of its initial concentration as y_0 ($y_0 > 0$), and the value
141 of c' can be obtained by solving Eq. (S10), which gives $c' = 1 - (y_0 \cdot a / b)$.

142 In the meantime, we also notice that, when t is infinitely large, the concentration of POZ
143 unlimitedly approaches a constant, which is denoted as y_∞ in Eq. (S22).

$$144 \quad y_\infty = \lim_{t \rightarrow \infty} \left[\frac{b}{a} \cdot (1 - c' e^{-at}) \right] = \frac{b}{a} \quad (S22)$$

145 We find it more convenient to express c' as $c' = 1 - (y_0 / y_\infty)$, so Eq. (S10) transforms into
146 a general expression of y , as shown in Eq. (S23).

$$147 \quad y = y_\infty \cdot \left[1 - \left(1 - \frac{y_0}{y_\infty} \right) \cdot e^{-at} \right] \quad (S23)$$

148 In this case, if we define the scale factor (s) as the ratio of the initial POZ concentration to
149 its ultimate value at an infinite t (i.e., $s = y_0 / y_\infty$ and $s > 0$), and transform y_∞ , a and b back to their
150 original symbols, the analytical expression of C_{POZ} incorporating the scale factor will be given by
151 Eq. (S24).

$$152 \quad C_{POZ} = k_1 \cdot p \cdot \left(\frac{1}{k_{-2} + k_3} \right) \cdot \left(\frac{k_2}{k_{-1} + k_2} \right) \cdot \left[1 - (1 - s) \cdot e^{-(k_{-2} + k_3)t} \right] \quad (S24)$$

153 Considering the formation of all the POZs and their CIs, along with the approximations
154 discussed in Text S1, we further obtain the analytical expression of k_{CI} that accounts for the pre-
155 existing POZs, as given by Eq. (S25).

$$156 \quad k_{CI} \approx k_{oz} \cdot \sum_i \{ r_i \cdot [1 - (1 - s_i) \cdot e^{-k_{3,i}t}] \} \quad (S25)$$

157 Thus, the analytical expression of $f_{CI,i}$ becomes Eq. (S26).

158
$$f_{CI,i} = r_i \cdot [1 - (1 - s_i) \cdot e^{-k_{3,i}t}] \quad (S26)$$

159 Eqs. (S25) and (S26) show that, when the ozonolysis begins (i.e., $t = 0$), the value of $f_{CI,i}$ is
 160 no longer zero but $r_i \cdot s_i$. Such a difference reveals that, if the i -th POZ pre-exists, the initial
 161 formation rate constant of the i -th CI is not yet zero. As s_i in Eq. (S26) is not considered as a time-
 162 independent quantity in this kinetic study, the value of k_{CI} with pre-existing POZs will unlimitedly
 163 approach k_{oz} if the t is infinitely large (Eq. (S27)).

164
$$\begin{aligned} \lim_{t \rightarrow \infty} k_{CI}(t, T) &\approx \lim_{t \rightarrow \infty} [k_{oz}(T) \cdot \sum_i f_{CI,i}(t, T)] \\ 165 &= k_{oz}(T) \cdot \lim_{t \rightarrow \infty} \sum_i f_{CI,i}(t, T) \\ 166 &= k_{oz}(T) \cdot \lim_{t \rightarrow \infty} \sum_i \{r_i \cdot [1 - (1 - s_i) \cdot e^{-k_{3,i}t}]\} \\ 167 &= k_{oz}(T) \cdot \sum_i r_i \\ 168 &= k_{oz}(T) \end{aligned} \quad (S27)$$

169 Eqs. (S26) and (S27) indicate that, although pre-existing POZs may help reduce the gap
 170 between k_{CI} and k_{oz} , k_{CI} is still deviated from k_{oz} . We should be cautious about using k_{oz} to represent
 171 k_{CI} in the modeling of CI formation.

172

173 **Table S1.** Fitted pre-exponential factors (A) of the Arrhenius equation based on the computational
 174 results of k_{-1} and k_2 for each SPC generated from the ozonolysis of α -cedrene and α -copaene.

SPC	α -cedrene		α -copaene	
	k_{-1}	k_2	k_{-1}	k_2
SPC1-1	1.6×10^{13}	4.2×10^{10}	1.6×10^{13}	9.3×10^9
SPC1-2	1.6×10^{13}	2.1×10^{10}	1.6×10^{13}	7.9×10^9
SPC2-1	1.6×10^{13}	2.1×10^{10}	1.6×10^{13}	5.7×10^{13}
SPC2-2	1.6×10^{13}	1.7×10^{10}	1.6×10^{13}	1.5×10^{13}

175

176 **Table S2.** Branching ratio of the ozonolysis channels of α -cedrene and α -copaene corresponding
 177 to different SPCs across the studied temperatures.

T (K)	α -cedrene ozonolysis				α -copaene ozonolysis			
	1-1	1-2	2-1	2-2	1-1	1-2	2-1	2-2
243	0.00	0.00	0.94	0.06	0.00	0.00	0.66	0.34
248	0.00	0.00	0.94	0.06	0.00	0.00	0.65	0.35
253	0.00	0.00	0.93	0.07	0.00	0.00	0.65	0.35
258	0.00	0.00	0.93	0.07	0.00	0.00	0.64	0.36
263	0.00	0.00	0.93	0.07	0.00	0.00	0.63	0.37
268	0.00	0.00	0.93	0.07	0.00	0.00	0.63	0.37
273	0.00	0.00	0.92	0.08	0.00	0.00	0.62	0.38
278	0.00	0.00	0.92	0.08	0.00	0.00	0.62	0.38
283	0.00	0.00	0.92	0.08	0.00	0.00	0.61	0.39
288	0.00	0.00	0.91	0.09	0.00	0.00	0.60	0.40
293	0.00	0.00	0.91	0.09	0.00	0.00	0.60	0.40
298	0.00	0.00	0.91	0.09	0.00	0.00	0.59	0.41
303	0.00	0.00	0.90	0.10	0.00	0.00	0.59	0.41
308	0.00	0.00	0.90	0.10	0.00	0.00	0.59	0.41
313	0.00	0.00	0.90	0.10	0.00	0.00	0.58	0.42
318	0.00	0.00	0.90	0.10	0.00	0.00	0.58	0.42
323	0.00	0.00	0.89	0.11	0.00	0.00	0.57	0.43

178

179 **Table S3.** Relaxation timescale of CI formation from the ozonolysis of α -farnesene and β -
 180 farnesene.

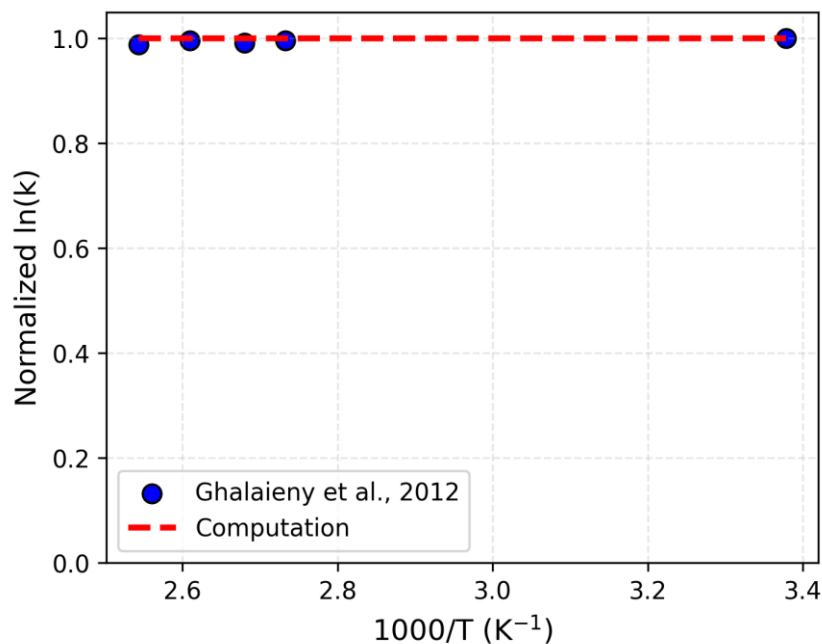
T (K)	α -farnesene (unit: minutes)		β -farnesene (unit: minutes)	
	CI1	CI2	CI1	CI2
243	0.4	7.1	556.3	483.9
248	0.2	3.5	276.1	210.7
253	0.1	1.8	140.8	94.7
258	0.1	0.9	73.7	43.9
263	0.0	0.5	39.5	20.9
268	0.0	0.3	21.7	10.3
273	0.0	0.2	12.1	5.2
278	0.0	0.1	7.0	2.7
283	0.0	0.1	4.1	1.4
288	0.0	0.0	2.4	0.8
293	0.0	0.0	1.5	0.4
298	0.0	0.0	0.9	0.2
303	0.0	0.0	0.6	0.1
308	0.0	0.0	0.4	0.1
313	0.0	0.0	0.2	0.0
318	0.0	0.0	0.1	0.0
323	0.0	0.0	0.1	0.0

181

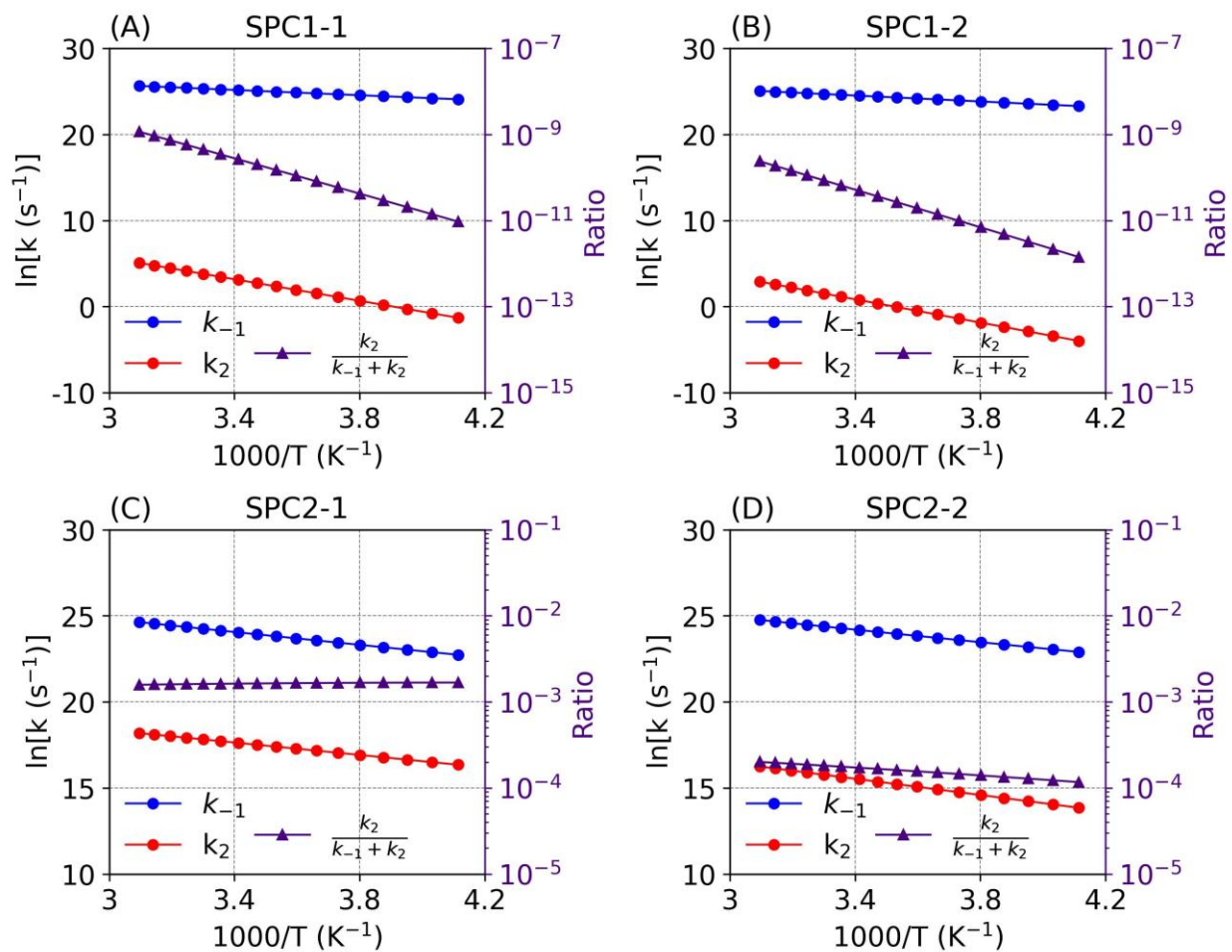
182 **Table S4.** Comparison of computed POZ decomposition energy barriers between DLPNO-
183 CCSD(T)/def2-TZVPP and DLPNO-CCSD(T)/cc-pVTZ (unit: kcal mol⁻¹).

Sesquiterpenes	DLPNO-CCSD(T)/def2-TZVPP		DLPNO-CCSD(T)/cc-pVTZ	
	CI1	CI2	CI1	CI2
α -cedrene	15.2	18.3	15.6	18.7
α -copaene	21.4	22.9	21.8	23.2
β -caryophyllene	27.6	25.8	28.1	26.3
α -farnesene	15.6	16.2	15.9	16.5
β -farnesene	16.4	19.2	16.9	19.5

184



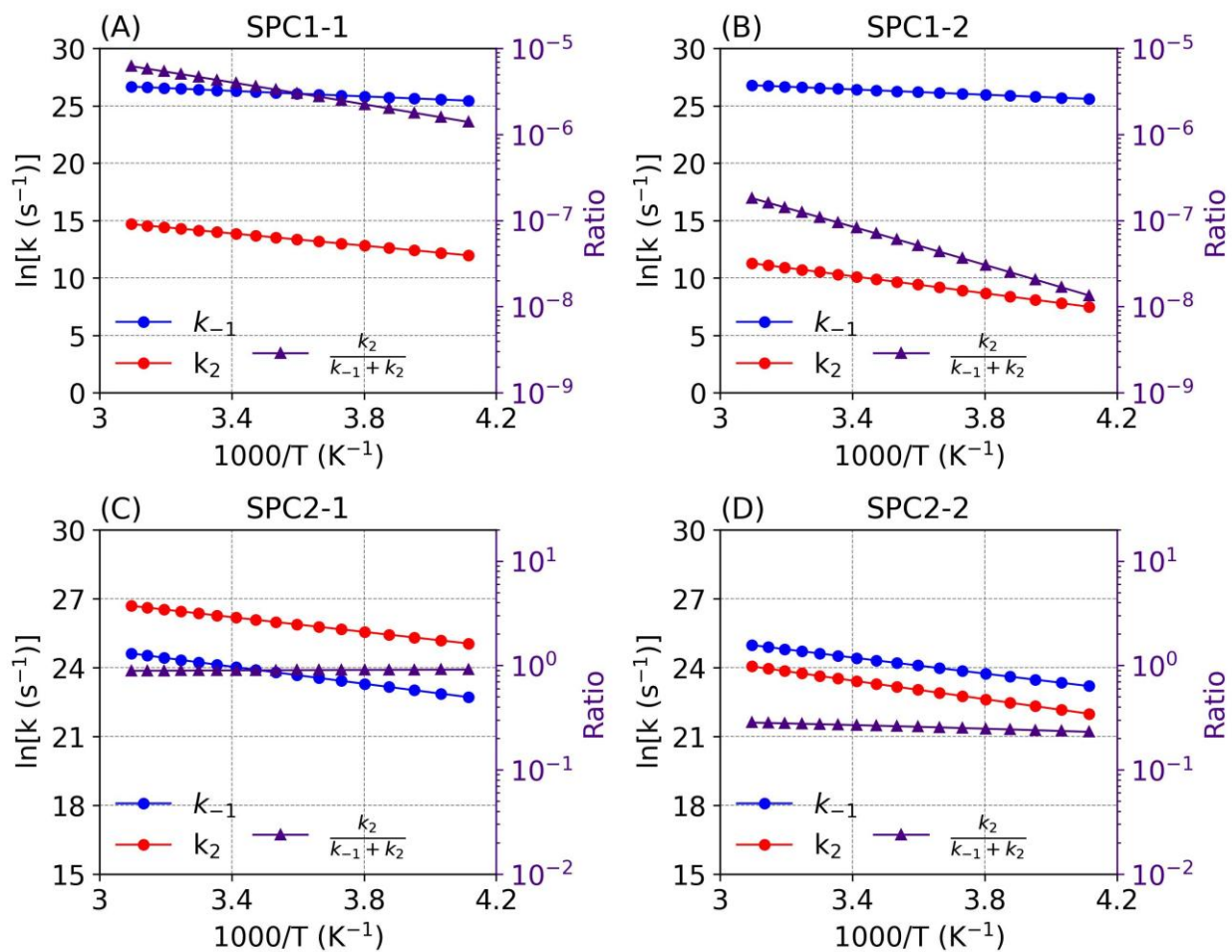
185
186 **Figure S1.** The experimental and computed ozonolysis rate constant of α -cedrene at different
187 temperatures. The experimental data is reproduced with permission (Ghalaieny et al., 2012).
188 Copyright 2012 Royal Society of Chemistry.
189



190

191 **Figure S2.** Temperature dependence of $\ln(k_{-1})$, $\ln(k_2)$ and $k_2 / (k_{-1} + k_2)$ of α -cedrene ozonolysis.

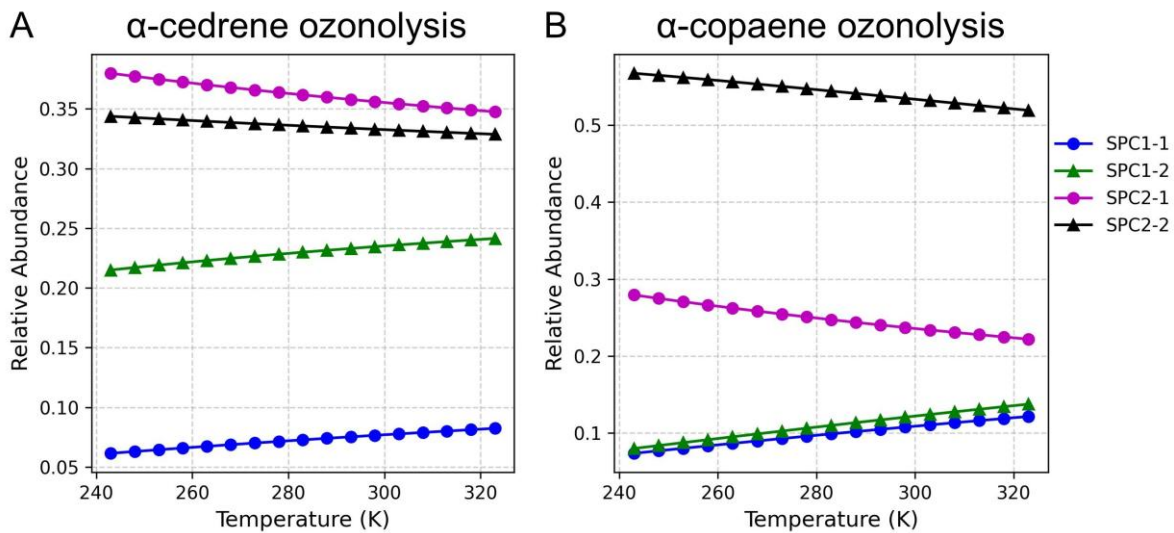
192



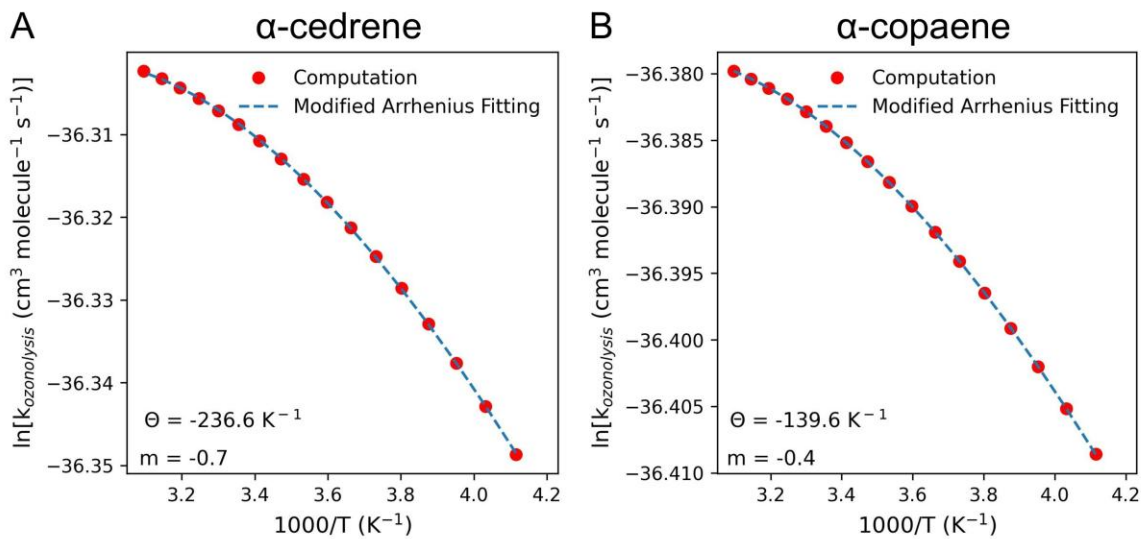
193

194 **Figure S3.** Temperature dependence of $\ln(k_{-1})$, $\ln(k_2)$ and $k_2 / (k_{-1} + k_2)$ of α -copaene ozonolysis.

195



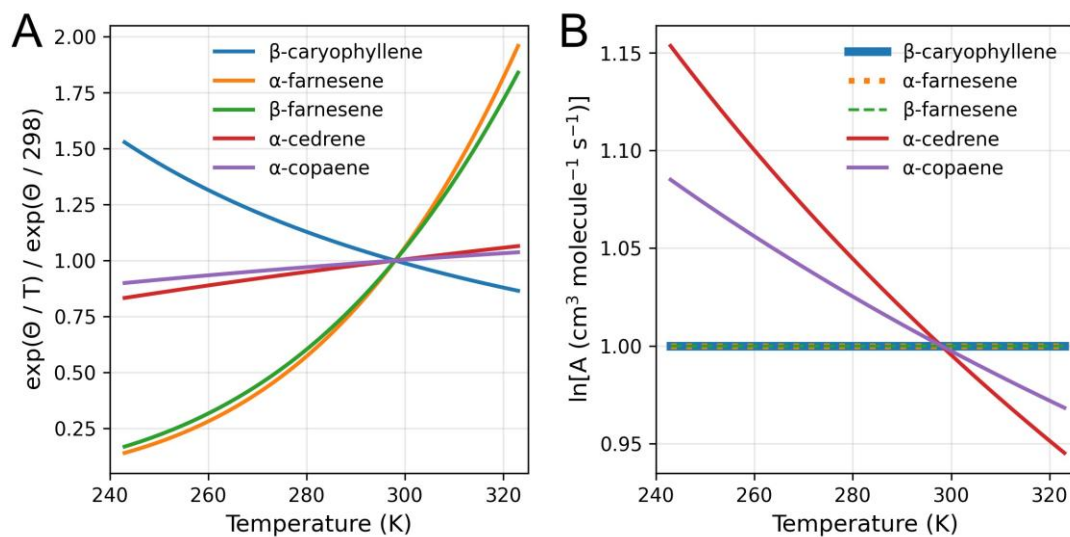
196
 197 **Figure S4.** The relative abundance of SPCs in the ozonolysis of (A) α -cedrene and (B) α -copaene
 198 across the studied temperatures.
 199



200

201 **Figure S5.** Fitting of the computed temperature-dependent ozonolysis rate constants with the
 202 modified Arrhenius equation.

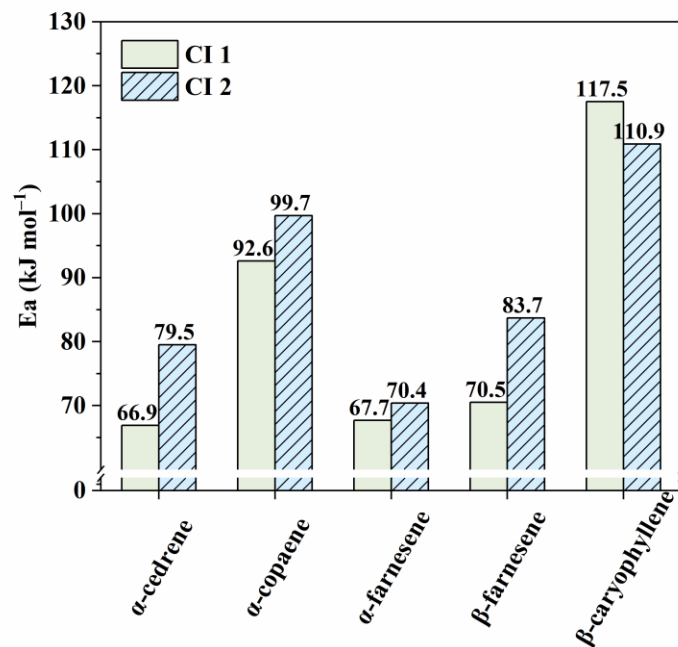
203



204

205 **Figure S6.** Comparison of Arrhenius equation components among β -caryophyllene (Gao et al.,
 206 2022), α -farnesene (Kim et al., 2011), β -farnesene (Kim et al., 2011), α -cedrene, and α -copaene:
 207 (A) relative exponential factor, and (B) pre-exponential factor (natural logarithm).

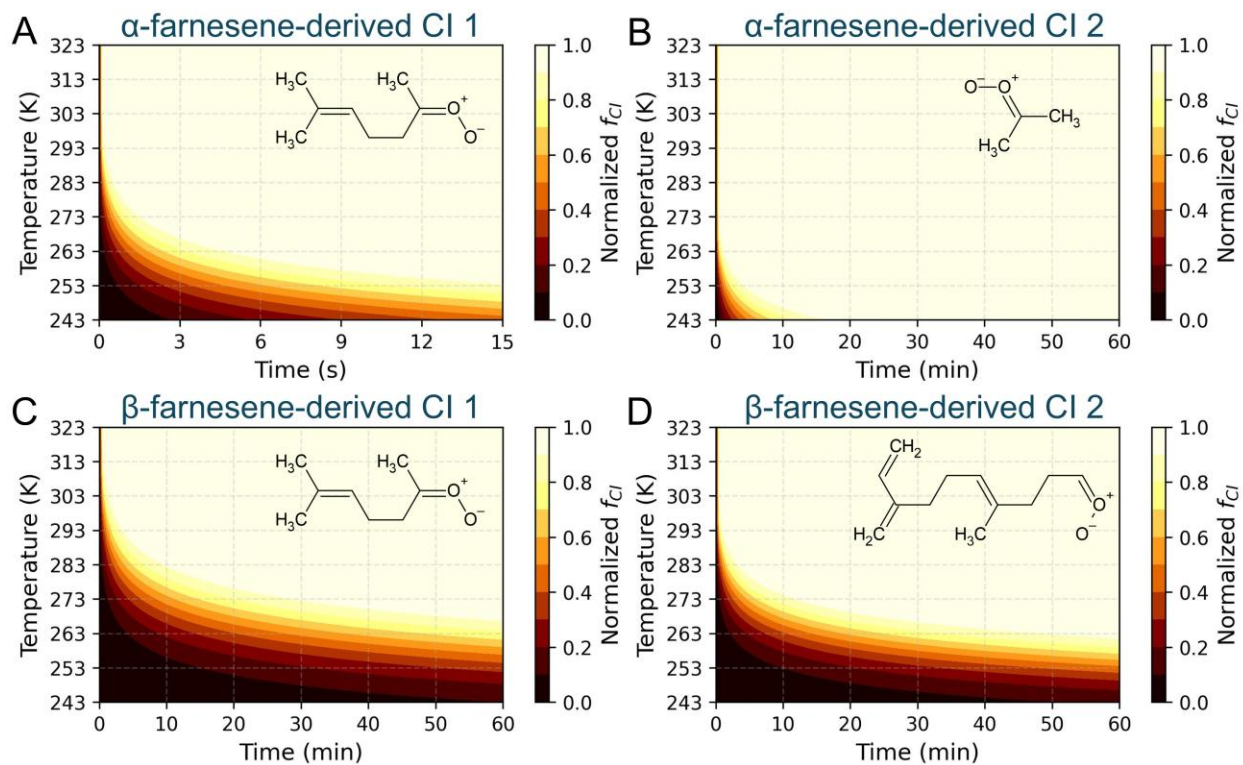
208



209

210 **Figure S7.** Activation energy of POZ decomposition rate constants (k_3) corresponding to CI1 and
 211 CI2 of all the studied sesquiterpenes.

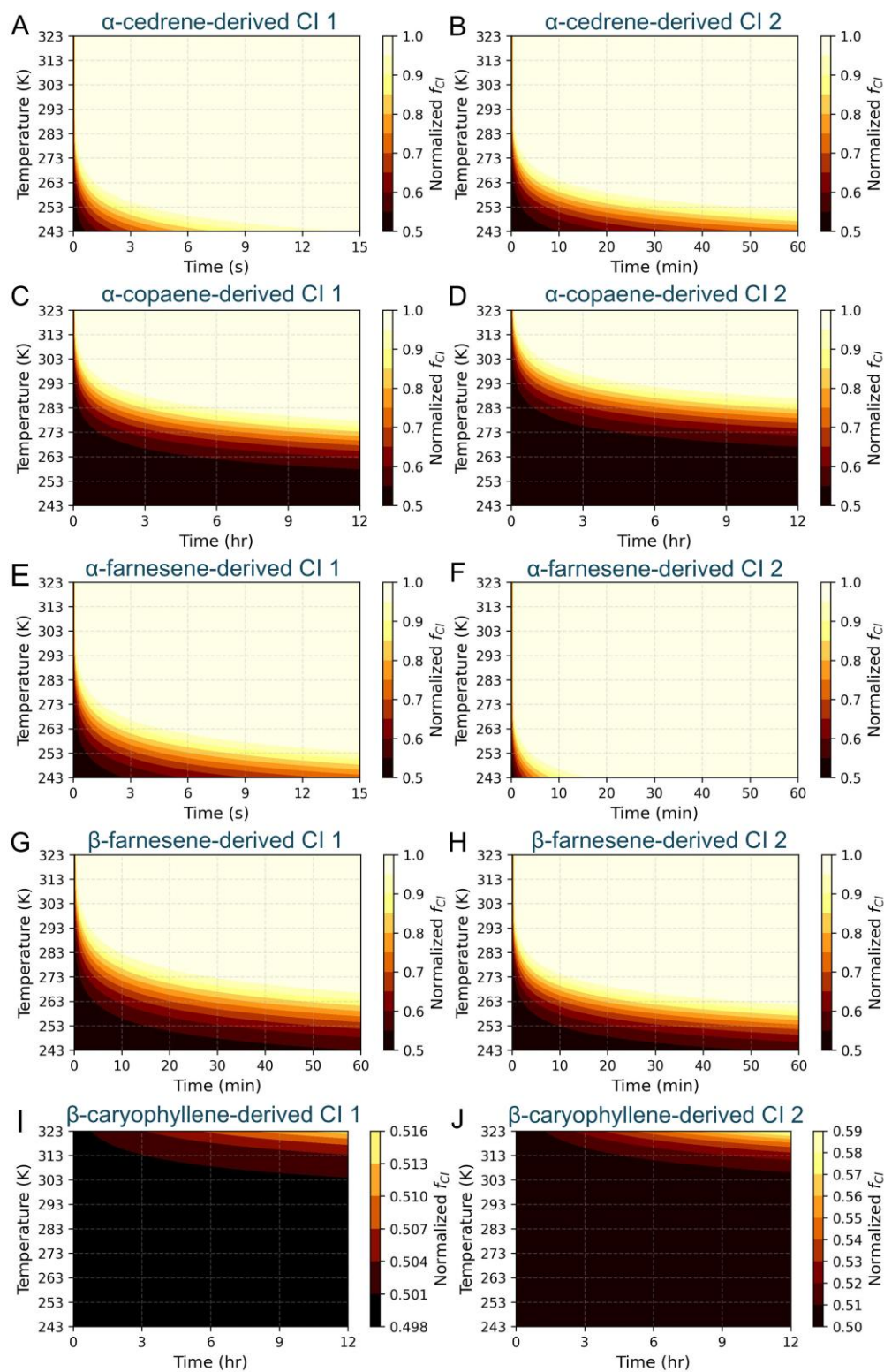
212



213

214 **Figure S8.** Kinetic relaxation of formation rate constant of (A) α -farnesene-derived CI1; (B) α -
 215 farnesene-derived CI2; (C) β -farnesene-derived CI1; (D) β -farnesene-derived CI2.

216



217

218 **Figure S9.** Kinetic relaxation of the modified k_{CI} with a scale factor of 0.5 for all the studied
 219 sesquiterpenes.

220

221 **References**

- 222 Davis, M. E., Drake, W., Vimal, D., and Stevens, P. S.: Experimental and theoretical studies of
223 the kinetics of the reactions of OH and OD with acetone and acetone-d6 at low pressure, J.
224 Photochem. Photobiol. A Chem., 176, 162-171, <https://doi.org/10.1016/j.jphotochem.2005.08.030>,
225 2005.
- 226 Donahue, N. M., Drozd, G. T., Epstein, S. A., Presto, A. A., and Kroll, J. H.: Adventures in
227 ozoneland: down the rabbit-hole, Phys. Chem. Chem. Phys., 13, 10848-10857,
228 10.1039/C0CP02564J, 2011.
- 229 Gao, L., Song, J., Mohr, C., Huang, W., Vallon, M., Jiang, F., Leisner, T., and Saathoff, H.:
230 Kinetics, SOA yields, and chemical composition of secondary organic aerosol from β -
231 caryophyllene ozonolysis with and without nitrogen oxides between 213 and 313 K, Atmos. Chem.
232 Phys., 22, 6001-6020, 10.5194/acp-22-6001-2022, 2022.
- 233 Ghalaieny, M., Bacak, A., McGillen, M., Martin, D., Knights, A. V., O'Doherty, S., Shallcross, D.
234 E., and Percival, C. J.: Determination of gas-phase ozonolysis rate coefficients of a number of
235 sesquiterpenes at elevated temperatures using the relative rate method, Phys. Chem. Chem. Phys.,
236 14, 6596-6602, 10.1039/C2CP23988D, 2012.
- 237 Kim, D., Stevens, P. S., and Hites, R. A.: Rate Constants for the Gas-Phase Reactions of OH and
238 O₃ with β -Ocimene, β -Myrcene, and α - and β -Farnesene as a Function of Temperature, J. Phys.
239 Chem. A, 115, 500-506, 10.1021/jp111173s, 2011.
- 240 Ou, H. and Chen, K.: Atmospheric Temperature Dependence of β -Caryophyllene Ozonolysis
241 Kinetics Is Governed by Stabilized Prereactive Complexes, J. Phys. Chem. A, 129, 9982-9990,
242 10.1021/acs.jpca.5c05523, 2025.
- 243 Taatjes, C. A., Shallcross, D. E., and Percival, C. J.: Research frontiers in the chemistry of Criegee
244 intermediates and tropospheric ozonolysis, Phys. Chem. Chem. Phys., 16, 1704-1718,
245 10.1039/C3CP52842A, 2014.
- 246 Talukdar, R. K., Gierczak, T., McCabe, D. C., and Ravishankara, A. R.: Reaction of Hydroxyl
247 Radical with Acetone. 2. Products and Reaction Mechanism, J. Phys. Chem. A, 107, 5021-5032,
248 10.1021/jp0273023, 2003.
- 249 Vereecken, L. and Francisco, J. S.: Theoretical studies of atmospheric reaction mechanisms in the
250 troposphere, Chem. Soc. Rev., 41, 6259-6293, 10.1039/C2CS35070J, 2012.

251